Estimating battery lifetimes in Solar Home System design using a practical modelling methodology

Narayan, Nishant; Papakosta, Thekla; Vega-Garita, Victor; Qin, Zian; Popovic-Gerber, Jelena; Bauer, Pavol; Zeman, Miroslav

DOI
10.1016/j.apenergy.2018.06.152

Publication date
2018

Document Version
Final published version

Published in
Applied Energy

Citation (APA)
Narayan, N., Papakosta, T., Vega-Garita, V., Qin, Z., Popovic-Gerber, J., Bauer, P., & Zeman, M. (2018). Estimating battery lifetimes in Solar Home System design using a practical modelling methodology. *Applied Energy*, *228*, 1629-1639. https://doi.org/10.1016/j.apenergy.2018.06.152

Applied Energy 228 (2018) 1629–1639

Contents lists available at ScienceDirect

Applied Energy

journal homepage: www.elsevier.com/locate/apenergy

Estimating battery lifetimes in Solar Home System design using a practical modelling methodology

Nishant Narayan*, Thekla Papakosta, Victor Vega-Garita, Zian Qin, Jelena Popovic-Gerber, Pavol Bauer, Miroslav Zeman

Department of Electrical Sustainable Energy, Delft University of Technology, Mekelweg 4, 2628 CD Delft, The Netherlands

HIGHLIGHTS

- The proposed methodology is independent of battery chemistries.
- The methodology is developed for Solar Home Systems (SHS) application in rural areas.
- The dynamic capacity fading model is highly practical and accurate.
- Comparison with empirical model for LiFePO4 battery shows a very close match.
- Methodology can be very useful for SHS designers for battery sizing.

ARTICLE INFO

Keywords:
Dynamic battery lifetime estimation
Cyclic ageing
Battery lifetime model
Battery sizing
Solar Home Systems

ABSTRACT

The rapid increase in the adoption of Solar Home Systems (SHS) in recent times hopes to ameliorate the global problem of energy poverty. The battery is a vital but usually the most expensive part of an SHS; owing to the least lifetime among other SHS components, it is also the first to fail. Estimating battery lifetime is a critical task for SHS design. However, it is also a complex task due to the reliance on experimental data or modelling cell level electrochemical phenomena for specific battery technologies and application use-case. Another challenge is that the existing electrochemical models are not application-specific to Solar Home Systems. This paper presents a practical, non-empirical battery lifetime estimation methodology specific to the application and the available candidate battery choices. An application-specific SHS simulation is carried out, and the battery activity is analyzed. A practical dynamic battery lifetime estimation method is introduced, which captures the fading capacity of the battery dynamically through every micro-cycle. This method was compared with an overall non-empirical battery lifetime estimation method, and the dynamic lifetime estimation method was found to be more conservative but practical. Cyclic ageing of the battery was thus quantified and the relative lifetimes of 4 battery technologies are compared, viz. Lead-acid gel, Flooded lead-acid, Nickel-Cadmium (NiCd), and Lithium Iron Phosphate ($LiFePO_4$) battery. For the same SHS use-case, State-of-Health (SOH) estimations from an empirical model for $LiFePO_4$ is compared with those obtained from the described methodology, and the results are found to be within 2.8%. The relevance of this work in an SHS application is demonstrated through a delicate balance between battery sizing and lifetime. Based on the intended application and battery manufacturer's data, the practical methodology described in this paper can potentially help SHS designers in estimating battery lifetimes and therefore making optimal SHS design choices.

1. Introduction

An estimated 1.2 billion people around the world lacked access to electricity as of 2016, with almost 85% of this population living in the rural areas. Fig. 1 shows the distribution of the global population without electricity. For various reasons, most of these unelectrified regions and communities have not received grid-based electricity [1]. In the absence of a central grid as an imminent solution [2], Solar Home Systems (SHS) seem to be a promising route to address immediate electricity needs in the off-grid areas [3].

A Solar Home System is defined as a Photovoltaic (PV)-based generator usually rated between 50 Wp and 250 Wp, accompanied by a

* Corresponding author.
E-mail address: N.S.Narayan@tudelft.nl (N. Narayan).

https://doi.org/10.1016/j.apenergy.2018.06.152
Received 5 March 2018; Received in revised form 26 June 2018; Accepted 30 June 2018

Nomenclature

Variables

DOD	Depth of discharge
I	Current
t	Time
C	Battery capacity
T	Temperature
n	Cycle life
f	Linear factor
D_n	Difference in cycle life between two temperatures
$p_0 - p_4$,	Polynomial coefficients at reference temperature
p_{l_1}, p_{l_4}	Fitting coefficients for determining the linear factor
$p_{d_0} - p_{d_4}$	Fitting coefficients for differences between two temperature curves
d	Battery DOD
$\overline{DOD}$	Average DOD
$\overline{T}$	Average T
L	Lifetime in years
E_{thr}	Energy throughput
E_{nom}	Nominal battery energy capacity
α	Proportional number of cycles
D	Battery damage
E	Number of events until end of life is reached
cf	Capacity fading

Abbreviations

LLP	Loss of load probability
SHS	Solar home system(s)
ZC	Zero-crossing
SOC	State of charge
EOL	End of life
SOH	State of health
LA	Lead-acid
ref	Reference
avg	Average
dev	Deviation

suitable battery storage [5]. The term has mostly come to be used in the context of off-grid electrification, although sometimes it may be used interchangeably with a standalone PV system. The battery is a vital component of the SHS, enabling energy storage of the PV output. However, the sizable proportion of upfront battery costs makes the battery the most expensive SHS component, as seen in Fig. 2. This fact, coupled with the low battery lifetimes (sometimes even up to 3 years [5]), makes battery-costs the most relevant in SHS design. Battery-costs recur not just in terms of the upfront costs, but also in terms of the replacements during SHS lifetime, thereby making battery lifetime a critical parameter in SHS applications.

Additionally, the accurate sizing of the battery can impact the battery lifetime [1]. This is because an increase in battery size for the same application reduces the average Depth of Discharge (DOD) for the battery [7], as seen below in Section 3. Therefore, the sizing of the battery in an SHS presents itself as an interesting balance between upfront costs (size) and lifetime [3].

Battery lifetime is thus seen as a vital parameter to be considered in SHS design, especially in the cost-sensitive context of the under-electrified communities.

1.1. Literature study

Battery lifetime estimation models can be broadly classified under two categories, viz. performance-based models and cycle counting models.

In performance-based models, the performance values of the battery are simulated based on certain performance parameters. When the particular parameter drops below a pre-determined value, the end of life (EOL) is reached for the battery. These can be classified into 4 different categories. (i) Electrochemical Models that need extensive information on the chemical and physical interactions occurring within the battery in order to accurately model the battery. Despite the efforts to simplify these models while effectively estimating the dynamically changing states (SOC and SOH) [8], the lack of detailed information such as Li-ion concentration, diffusion coefficients, reaction rates, ionic conductivity, reduce the applicability of these models specially when different battery technologies are to be compared. (ii) Equivalent Electrical Circuit Models that represent the battery as an equivalent electrical circuit comprising electrical elements like resistors, capacitors, voltage, and current sources. These kind of models can also include the thermal stresses related to fast charging to develop optimal charging profiles [9]. A combined electrochemical-thermal model has also helped in recent studies to develop health-aware strategies for fast charging of Li-ion battery, underlining the importance of being able to model SOH in battery applications [10]. (iii) Analytical Models with empirical data fitting are constructed by interpolating and fitting empirical data obtained through experiments. (iv) Artificial neural networks (ANN) can establish a relationship between the system outputs and input operating conditions, given a large enough dataset [11].

Performance-based models can rely on experimental methods that observe and measure the battery degradation through time, or on semi-empirical approaches that represent the fade mechanisms using equations that fit a particular type of cell. These models can also be constructed by including the physiochemical effects behind the side reactions of a particular set of chemical compounds endemic to particular cell chemistries. Therefore, the main limitation of all of the underlying

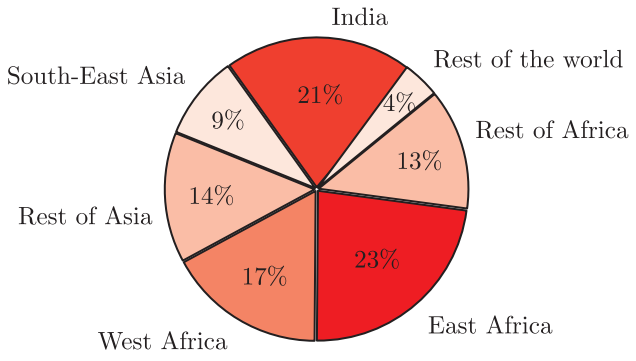

Fig. 1. Distribution of globally unelectrified population (data sourced from [4]).

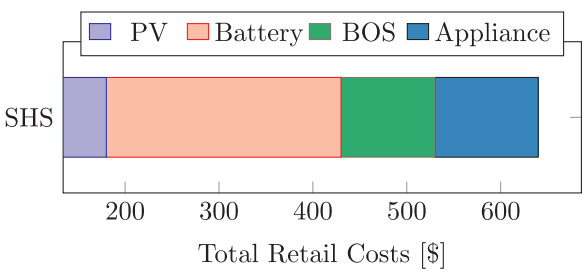

Fig. 2. Split-up of upfront costs of SHS components for powering a 19″ TV, radio, lights and a mobile phone charger in 2014 (data from [6]).

approaches for performance-based models is that they are constructed for specific cells, under certain environment conditions, and tested through a limited amount of time [12]. Additionally, some semi-empirical approaches do not consider the effect of parameters like DOD [13]. For models relying on ANN, a vast amount of data is first needed for the neural network to be trained reliably. In general, it can be said that to construct reliable performance-based models, it not only costs time per specific intended application and use-case needed but also raises concerns on the accuracy of these approaches if they were to be used under a different set of conditions wherein the same battery technology undergoes a different stress pattern.

Unlike performance-based models, cycle counting or weighted Ah-throughput (charge processed by the battery) models are able to determine parameters which can be linked to their EOL, for e.g., Ah-throughput (the amount of energy processed by the battery), cycles, or time since manufacturing [11]. A comparison study in the past has shown accurate results for lifetime prediction with weighted Ah-throughput model [14]. These models are mainly based on the data provided by the manufacturers, assuming that the battery is able to achieve an overall Ah-throughput throughout its life under certain specific stress factors like DOD and temperature. Palmgren-Miner (PM) rule is one of the most common examples that fit in the category of cycle counting models. The different lifetime estimation models are compared in Table 1.

There have been a few cycle-counting based lifetime estimation models discussed in the past [15–17], most notably [3], where the authors discuss a simple methodology for non-empirical battery lifetime estimation. However, while [15] assumes an arbitrary duration of a cycling event 6400 s long, [16] uses only temperature as a stress factor but not for battery storage specifically, [17] employs off-line cycle-counting through rainflow counting algorithm but using DOD as the only stress factor for battery degradation, and [3] does not take into account dynamic capacity fading and temperature as an additional stress factor. Ref. [18] presents a lifetime estimation of lead-acid battery, but also does not consider dynamic capacity fading, and the capacity loss is only estimated after one entire year of simulation using rainflow counting algorithm.

This paper focuses on a non-empirical, cycle-counting approach for the estimation of the battery lifetime while also taking into account important battery stress factors like DOD and temperature. Given the off-grid SHS application, where the typical battery C-rates are C/20 to C/10 [19,20], the C-rates are considered to be low enough to not be included as a critical stress factor. The dynamic capacity fading model proposed here is capable of estimating the State of Health (SOH) after every micro-cycle based degradation while the battery is under operation. Additionally, multiple technologies are used in this study, demonstrating the usefulness of the proposed methodology across multiple battery technologies without having to model the electrochemical processes at the cell level for the different technologies.

1.2. Contributions of this paper

Following are the main contributions of this paper.

- A methodology to estimate the battery lifetime in a practical way using the application-based, expected battery usage and the battery data provided by the manufacturer. The methodology is applicable across battery technologies.
- Insight into performance of 4 different battery technologies for the SHS application.
- A dynamic capacity fading model that quantifies the fractional degradation caused by the micro-cycles of battery activity.
- Finally, insight into the impact of battery sizing on estimating battery lifetime, underlining the relevance of battery lifetime estimation in SHS design.

2. Battery lifetime

2.1. Battery parameters

Some of the important battery parameters that this work refers to are discussed in this section.

State of Charge and Depth of Discharge. The state of charge (SOC) indicates battery charge as a fraction of the initial capacity, while the depth of discharge (DOD) refers to the capacity discharged as a fraction of the initial capacity. They are treated as a complement of each other.

The DOD can be calculated from the battery discharge current over a discharging interval as shown in Eq. (1).

$$DOD = \frac{\int_{t_i}^{t_f} I_{discharge}.\, dt}{C_i} \tag{1}$$

where t_f is the time at the end of the discharge interval process, t_i is the initial time, $I_{discharge}$ is the current, and C_i the initial battery capacity.

Cycle-life. Cycle-life is defined as the number of charge/discharge cycles that a battery can undergo maintaining a specified percentage of its initial capacity, after which batteries reach the end of life (EOL). The EOL is usually defined as 80% of the initial rated battery capacity [21].

State of Health (SOH). State of Health refers to the fraction of the rated battery capacity actually available for cycling. As the battery ages, the SOH reduces, and 80% SOH is often defined as the EOL for a battery.

The battery ageing can be classified into two categories.

Cyclic ageing. Cyclic ageing is related to the decrease in battery capacity while the battery is undergoing cycling. Cyclic ageing plays a larger role in cases where operation times are relatively longer than idle periods, like in off-grid SHS.

Calendar ageing. Calendar ageing is related to the decrease in battery capacity while the battery is under storage and not in use, and therefore, independent of charge/discharge cycles. Calendar ageing plays a

Table 1
Comparison of the performance-based and cycle-counting models in the context of battery life estimation. Adapted from [11].

Model type	Model example	Merits	Demerits
Performance based	Electro-chemical	Very high accuracy	Complex Low-speed
	Equivalent Electrical Circuit Model	Good prediction of dynamic behaviour	Depends on experimental data for accuracy Not suitable for lifetime prediction as is
	Analytical model with empirical data fitting	Ease of simulation using the model due to the analytical functions Good accuracy	Effects of various stress factors need to be combined from the experimental data Large amount of data needed
	Artificial Neural Networks (ANN)	Reasonable accuracy with high speed Knowledge of battery mechanisms not needed	Adequate training of ANN requires a large dataset
Cycle-counting	Palmgren-Miner	Deviations from standard operating conditions captured well Simple implementation	Although non-empirical in itself, relies on empirical data from the manufacturer

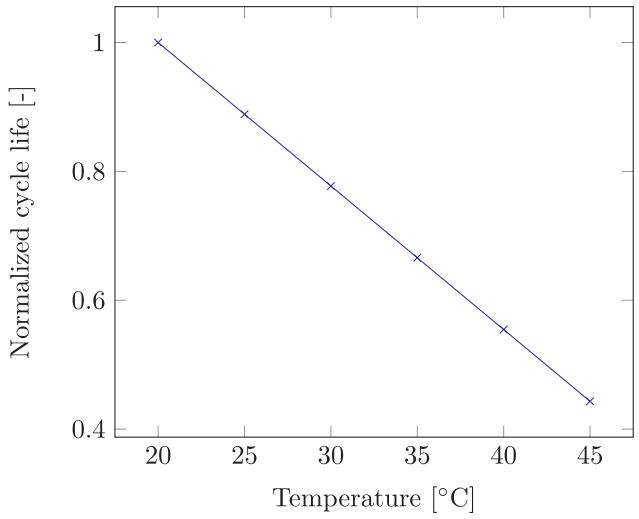

Fig. 3. Normalized cycle life with temperature for a flooded lead-acid battery at 30% DOD with a reference temperature of 20 °C. Data sourced from [30]).

predominant role in cases where operation times are shorter than idle periods [22].

This work takes into account only the cyclic ageing process. In other words, this work models the application-specific, battery induced capacity fading and the resulting battery lifetime.

Active SOC/DOD. Active SOC/DOD refers to the State-of-Charge or Depth-of-Discharge of the battery while the battery is in operation [3]. The concept of active SOC/DOD helps in looking at only those SOC/DOD points that actively contribute towards cyclic ageing of a battery, which is the focus of this work.

2.2. Causes of battery degradation

The loss of active lithium, principally at the anode, is the main reason for lithium-ion cell degradation. The mechanical stresses induced by cycling and temperature gradients lead to contraction and expansion, eventually increasing the cell impedance and reducing the cell capacity [22]. Electrode pore clogging, passive layer growth, and lithium metal plating are consequences of the undesired side reaction that takes place inside the Lithium-ion cells [23]. In the case of lead-acid batteries, the major degradation processes that decrease performance and provoke end of service life are anodic corrosion, active mass degradation, and loss of adherence to the grid [24]. Furthermore, the continuous loss of water in vented cells and the production of lead sulphate (in the electrodes) out of the active materials of the cell facilitates the ageing process [25]. NiCd cells suffer from hydrogen production when overcharged and when exposed to a temperature higher than nominal temperature; therefore, the accurate detection of the end-of-charge process is fundamental to avoid battery damage [26]. In NiCd cells, Cd crystallization happens under particular cycling and storage conditions, causing a reduction of active material while reducing the active surface dedicated to the electrochemical reaction [21].

Battery lifetime is directly related to battery usage, and therefore the way in which the battery cycling occurs and the environmental conditions affect the natural ageing of batteries. One of the principal factors to take into account is the DOD range of operation, which defines the usable capacity of the battery, and therefore, the battery range of operation. Another parameter that profoundly impacts battery ageing is cell temperature, where an increase in temperature translates into a higher electrochemical activity that instantaneously improves cell performance but in the long term fosters side reactions that consume the active materials, thereby diminishing battery capacity [27]. The kinetics of the electrochemical reaction also relates to the charge and discharge rates imposed by the applications. Therefore, the methodology introduced in the next section takes into account the influence of temperature and cycling to quantify their impact on lifetime.

3. Methodology

The methodology followed in this study is composed of multiple steps. Section 3.1 describes the extraction of lifetime data from the battery datasheet as a function of temperature and DOD. Section 3.2 details the SHS-based inputs used in the methodology. Sections 3.3 and 3.4 discuss the two models that are proposed and used in this study, viz. the overall battery usage model and the dynamic capacity fading model.

3.1. Battery data from the manufacturer

Battery manufacturers usually provide the battery cycle-life characteristics as a function of DOD and temperature, for e.g., [28]. The data from these curves are extracted, and lookup-functions are created.

Battery technology. Four different battery technologies are chosen for this study, viz., sealed Lead-Acid or Lead-Acid gel (LA-gel), Lithium-Iron Phosphate ($LiFePO_4$), flooded Lead-Acid (LA), and Nickel-Cadmium (NiCd) battery. The corresponding datasheets used are [28–31] respectively. While the merits and demerits of using one battery technology over the other for SHS application is a different subject of discussion altogether, the reason for including these different technologies in this study is to illustrate the usefulness of the described methodology to estimate the battery lifetime irrespective of the underlying battery chemistry.

Temperature linearity. For cycling at a given DOD level, it is observed that the cycle life shows a linear temperature dependency, at least in the range of 20–45 °C, a temperature range typically mentioned in the datasheets. This behaviour is illustrated in Fig. 3 for the flooded lead-acid battery.

Polynomial approximations. The linearity on temperature dependency is exploited to create polynomial approximation functions. A 4^{th} order polynomial approximation for the battery lifetime curves for the above-mentioned technologies is given by the following set of Equations.

$$n(T, DOD) = n(T_{\text{ref}}, DOD) - f(T_{\text{avg}}) D_n(DOD) \tag{2}$$

$$n(T_{\text{ref}}) = p_4 d^4 + p_3 d^3 + p_2 d^2 + p_1 d + p_0 \tag{3}$$

$$f = p_{l_1} T_{\text{avg}} + p_{l_0} \tag{4}$$

$$D_n = p_{d_4} d^4 + p_{d_3} d^3 + p_{d_2} d^2 + p_{d_1} d + p_{d_0} \tag{5}$$

where

$n(T, DOD)$=Cycle life for a given temperature and DOD
f=A linear factor
D_n = Difference of n between two temperatures
p_0 to p_4 = Polynomial fitting coefficients at T_{ref}
p_{l_1}, p_{l_0}=Fitting coefficients for determining the linear factor
p_{d_0} to p_{d_4}=Fitting coefficients for difference between two temperature curves
T_{avg}=Average operating temperature
T_{ref}=Reference operating temperature
d=Battery DOD

A reconstruction of the battery lifetime curves depending on temperature and DOD from the battery datasheet is shown in Fig. 4 for a flooded lead-acid battery. These curves are then approximated as polynomial 'lookup' functions that can be used in battery lifetime estimation based on the application-specific battery usage.

It must be noted that many manufacturers do not explicitly distinguish between the ambient temperature and the actual battery

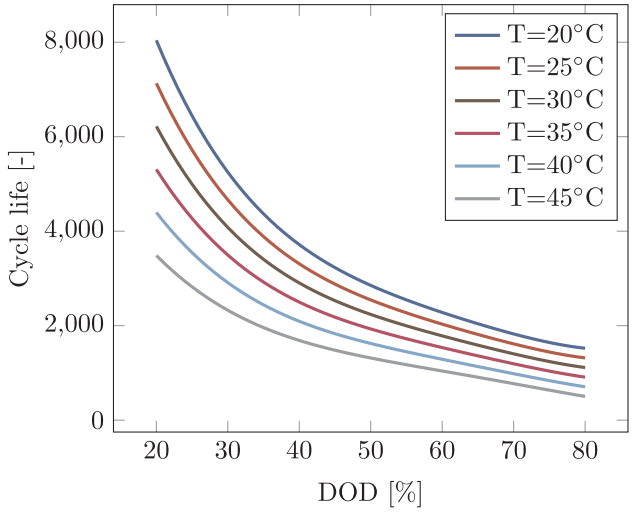

Fig. 4. Reconstruction of battery cycle-life curves based on DOD for flooded lead-acid battery (data sourced from [30]).

operating temperature, and some even mention the battery cycle-life curves at ambient temperature [30,28]. It is difficult to accurately determine the battery temperature, as it depends on several local operating conditions outside the electrical functioning of the system. In this study, the battery operating temperatures are taken to be at ambient levels, especially given the slow C-rates for the SHS batteries.

3.2. SHS application and load profile

A Solar Home System application was considered as the use-case for estimating the battery lifetime.

3.2.1. Load profile

A load profile was constructed based on estimating the electrical needs of a Tier 3 household [32] and inputs from the field [7], especially taking into account the efficient DC appliances that are on the rise in the off-grid market. Several works in the recent past have indicated a sharp rise in the availability as well as popularity of the so-called super-efficient DC appliances [6,33,34]. The operational (DC) loads that make up the load profile are LED lights, mobile phone charging, radio, TV, fridge, and a small computer. The load profile varies from day to day, with the average daily energy need being 1242 Wh. The daily load profile has been plotted for a given day in Fig. 5, along with the PV generation profile.

3.2.2. SHS PV size

The selected PV module is Jinko Solar JKM265P rated 265 Wp. One PV module is enough to cover the average daily energy needs for the given load profile. Additionally, the extra DC yield helps to compensate for the system inefficiencies. The PV output is modelled and corrected for thermal losses. The PV output is also shown for a single day in Fig. 5.

3.2.3. SHS battery size

Loss-of-Load probability (LLP) was chosen as the optimizing parameter for finding the desired battery size. LLP is a metric defined as the ratio of the expected amount of downtime (system failure) of the system while delivering the demanded power, to the total amount of time the system was designed to deliver power for. The concept of LLP has been explained in previous work in [7]. A battery size of 1440 Wh was considered for the given load profile and the chosen solar panel. This PV-battery combination guaranteed an LLP of 1.8% for the given load profile, i.e., this was the minimum storage size with the required PV size that could guarantee a total loss of load of 1.8% throughout the 1 year of simulation. The LLP optimization approach for the given load profile can be seen in Fig. 6.

3.2.4. SHS simulation

A simple model was constructed in MATLAB to simulate the functioning of the SHS for a year. The meteorological inputs to the model were obtained from the tool Meteonorm [35], which includes irradiance, wind speed and temperature. A sample geographical location experiencing an average of 5.5 equivalent sun hours per day was considered. The data resolution of the inputs to the model was 1-min. Although far from instantaneous, it is assumed that a one-minute data resolution provides reasonable accuracy to incorporate the intermittency of the PV generation and the load profile. Based on the load profile and the modelled PV output, the simulation was run over an arbitrary calendar year to obtain the battery usage pattern. It should be noted that the battery was limited to a maximum DOD limit of 80% in the simulation. The battery efficiency was assumed to be constant throughout the simulation, and certain constant efficiencies were assumed after a comparative study based on literature [36–40]. The efficiencies assumed are 85%, 90%, 78%, 93%, for flooded LA, LA-gel, NiCd, and $LiFePO_4$ respectively. Additionally, a constant electronic power conversion efficiency of 95% was assumed for the SHS. These efficiency numbers can also be specifically changed depending on the data from the manufacturer or the choice of a particular battery for the application without impacting the efficacy of the described methodology.

3.3. Overall battery usage model

In the overall battery usage method, the lifetime is estimated based on the overall battery usage that is extracted from the 1-year SHS simulation. The main parameters for estimating the battery lifetime are the average DOD and average temperature in battery operation. These were derived from the battery usage in two different ways, viz. the coarse average DOD and the micro-cycle zero-crossings based approach.

3.3.1. Coarse average approach

This is the less computationally demanding approach of the two, where the required average DOD and temperature values are simply taken as the average of all the data points throughout the simulation, as shown in Eq. (6).

$$\overline{DOD} = \frac{\sum_{i=1}^{N} DOD_i}{N} \tag{6}$$

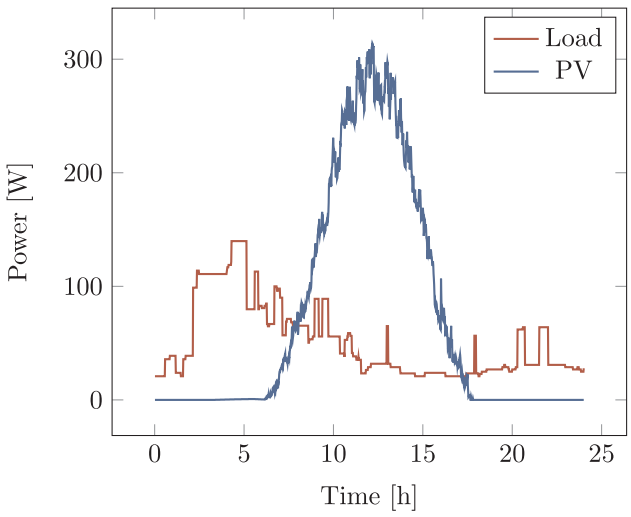

Fig. 5. One day load profile considered for a household with Tier 3 energy access, along with PV output for a single day.

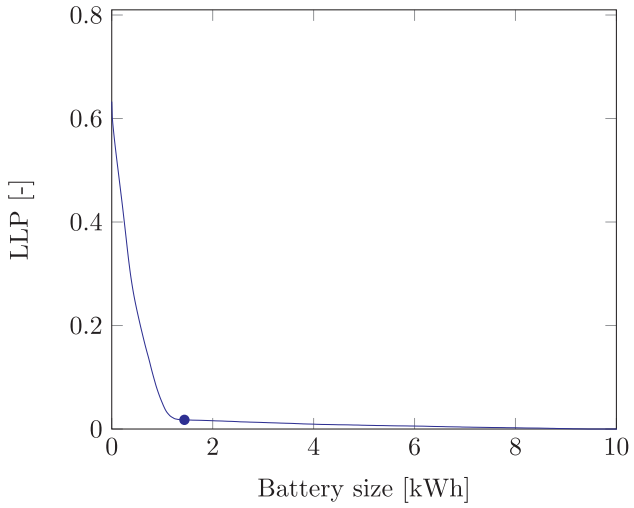

Fig. 6. Loss of load probability (LLP) curve for the given load profile with varying storage sizes. A battery size of 1440 Wh (marked on the graph) is deemed sufficient through this analysis, resulting in an LLP of 1.8%.

$$\overline{T} = \frac{\sum_{i=1}^{N} T_i}{N}$$

where $\overline{DOD}$ and $\overline{T}$ are the average DOD and temperature, N is the total number of data points in the simulation.

While computationally less intensive, a simple average does not capture the battery usage well. This is because not only does this method include the extraneous, inactive battery periods, but also the battery processes different amounts of energy throughput under different DODs. Therefore, a more weighted approach needs to be used for taking this into account.

3.3.2. Zero-crossing (ZC) approach

In the micro-cycle zero-crossing (ZC) approach, micro-cycles of battery activity are defined based on the zero-crossings of the battery current. Therefore, only the active battery cycling periods are considered. This concept was introduced in a recent publication from the authors [3].

A micro-cycle in this context is defined as a small cycle of variable duration that exists between two consecutive current zero crossings; this is typically much shorter than a full charge-discharge cycle. This method involves taking into account all the zero current transitions given the 1 min data resolution.

Fig. 7 illustrates this concept. In this case, the active DOD should only be considered for the durations that the battery is cycling. Therefore, the states with battery current $I_{\text{battery}} = 0$ are ignored. Note that the concept can be equivalently explained if the battery power P_{battery} is considered instead of I_{battery}. In that case, the area of each micro-cycle would give the energy that the battery cycles in that interval.

Finally, with the micro-cycle zero-crossing data extracted from the battery simulation, the average active DOD can be calculated as shown in Eq. (7).

$$\overline{DOD} = \frac{\sum_{i=1}^{N} \overline{DOD_i}.\, E_{thr_i}}{\sum_{i=1}^{N} E_{thr_i}} \tag{7}$$

where $\overline{DOD}$: Combined average active DOD due to all the micro-cycles, $\overline{DOD_i}$: Average active DOD in the i^{th} micro-cycle, E_{thr_i}: Total energy throughput in the i^{th} micro-cycle, N: total number of ZC-based micro-cycles.

The average temperature is calculated based on the duration of the ZCs as follows.

$$\overline{T} = \frac{\sum_{i=1}^{N} \overline{T_i}.\, T_{ZC_i}}{\sum_{i=1}^{N} T_{ZC_i}} \tag{8}$$

where $\overline{T}$: Combined average temperature due to all the micro-cycles, $\overline{T_i}$: Average temperature in the i^{th} micro-cycle, T_{ZC_i}: Total duration of the i^{th} micro-cycle.

3.3.3. Lifetime estimation based on overall battery usage

Once the $\overline{DOD}$ is known, the cycle-life number n is then obtained from the look-up functions described in Section 3.1. The battery lifetime is then estimated as shown in Eq. (9) below [3].

$$L = n \times \overline{DOD} \times \frac{2 \times E_{\text{nom}}}{\sum_{i=1}^{N} E_{thr_i}} \tag{9}$$

where (L) is the battery lifetime in years, and E_{nom} is the nominal battery energy capacity in Wh.

Assumptions under overall battery usage methodology. In the overall battery usage methodology, there are a few crucial assumptions that serve the balance between the complexity of implementation and accuracy. These are as follows.

1. The battery performs throughout the 1-year simulation without any loss in capacity.
2. The battery performance in terms of the dynamic SOC is irrespective of its SOH. That is, the SOC of the battery is not corrected for its faded capacity during the simulation.
3. Only one year of intended battery usage is enough to be able to linearly extrapolate the battery usage and hence the cycle life.

The major drawback of this method is that there is no loss in capacity of the battery during the simulation. Instead, the battery lifetime is estimated based on the overall battery usage for one year. It would be more accurate to estimate the battery lifetime while taking the capacity fading into account dynamically in the battery performance, as discussed in the next section.

3.4. Dynamic capacity fading model

The dynamic capacity model fundamentally differs from the overall battery usage method for battery lifetime estimation, in that this model dynamically assesses the damage caused due to the stress factors after every ZC micro-cycle. This model is implemented through a process explained in the flowchart illustrated in Fig. 8.

The SHS simulation starts as in the overall battery usage method, with SOH = 100%. The simulation is executed in 3 stages using the model. In Stage A, the battery activity is probed within the SHS simulation. Zero-crossings (ZCs) are recorded, and the capacity damage computations within this model start when the battery activity data is extracted for a ZC-based micro-cycle. This includes evaluating the

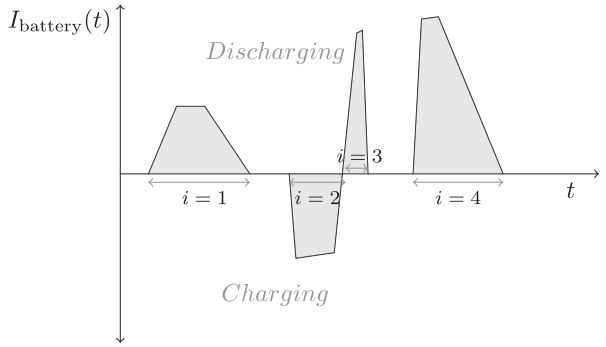

Fig. 7. An illustrative battery current waveform showing arbitrary micro-cycle intervals, where i is the micro-cycle number.

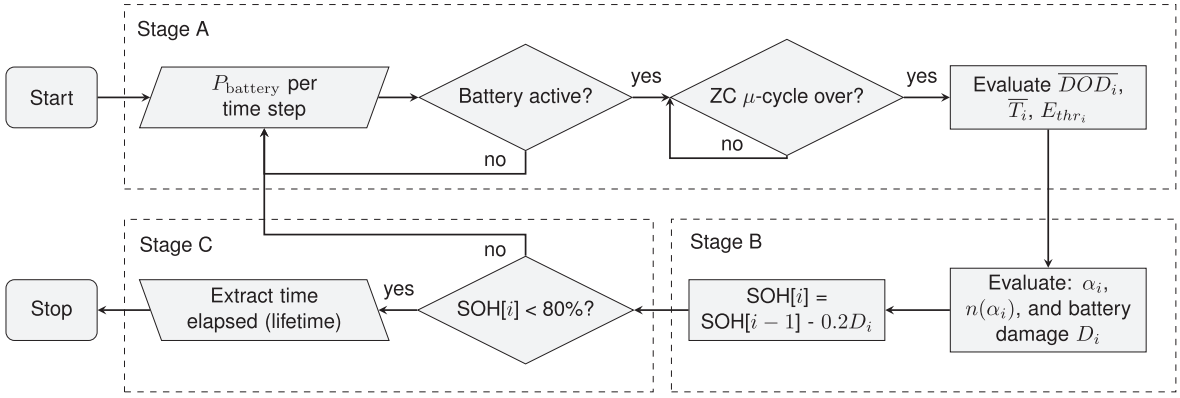

Fig. 8. Flowchart explaining the dynamic capacity fading model for lifetime estimation.

average battery DOD ($\overline{DOD_i}$), the energy throughput (E_{thr_i}) and the average temperature ($\overline{T_i}$) for the *i*th ZCs micro-cycle as shown in Eqs. (7) and (8).

In Stage B, the total number of cycles $n(\overline{T_i}, \overline{DOD_i})$ possible at the DOD and temperature levels is calculated using the polynomial lookup functions described in Section 3.1. Additionally, the proportional number of cycles ($\alpha_i(E_{thr_i}, E_{nom})$) spent under the same DOD and temperature levels for the *i*th ZCs micro-cycle is calculated as a function of the energy throughput (E_{thr_i}) and the nominal battery capacity (E_{nom}), as shown in Eq. (10).

$$\alpha_i = \frac{E_{thr_i}}{2 \times E_{\text{nom}} \times \overline{DOD_i}} \tag{10}$$

The damage (D_i) incurred to the battery life is then calculated using the Palmgren-Miner rule. This rule states that the lifetime of a component after undergoing a series of load events is reduced by a finite fraction corresponding to each of the load events. This fraction is the ratio between the number of cycles the element has undergone under a particular stress factor (or load event) to the total expected number of expected cycles until EOL under that stress factor [11,15]. Eq. (11) represents the Miner's rule.

$$D = \sum_{i=1}^{E} D_i = \sum_{i=1}^{E} \frac{\alpha_i}{n(\alpha_i)} \tag{11}$$

where α_i: number of cycles spent under a stress factor σ_i (DOD and temperature), $n(\alpha_i)$: total number of cycles for the EOL to be reached, E: number of events taken place until the EOL condition is reached, D: total damage accumulated, and D_i: damage at the battery for each one of these events. This damage is then scaled and subtracted from the current SOH. The damage scaling is done to ensure that when the total damage $D = 1$, the SOH is 80%.

Stage C involves checking for the EOL of the battery after every ZC micro-cycle of activity. If the SOH has reached 80% or below (or, in other words, if the damage D equals a value of 1.), the simulation ends, and the SOH data is extracted as a function of time. If SOH is $> 80\%$, the simulation continues in Stage A with the updated SOH. The stages repeat until the battery accumulates enough damage to reach its EOL. Note that the DOD values are all dynamic, i.e., the DOD values are computed based on the updated battery capacity after every micro-cycle.

3.4.1. Salient features of the dynamic capacity fading model

The dynamic capacity fading model is a significant upgrade over the overall battery usage model both in complexity and accuracy with which the micro-degradation per ZC micro-cycle is assessed. It has the following salient features.

1. **High resolution.** Given that the model captures the micro-cycle degradation, the dynamic capacity fading model serves with a high degree of resolution of the battery degradation. Thus, the model can potentially capture the micro-degradation in a time-step as small as the time resolution of the input data used for the application.
2. **Dynamic battery parameters** Battery parameters like DOD and SOC are updated after every ZC micro-cycle based on the degraded battery capacity. Therefore, the battery performance is not independent of the capacity fading.
3. **SOH estimation.** The model allows for SOH to be estimated after every micro-cycle, which is not possible with the overall battery usage model.
4. **Technology independent.** Given that the model is independent of electrochemical processes for its implementation, it can be used for any battery technology. In this study it is used to estimate the battery lifetime for 4 battery technologies.
5. **Application independent.** Without any loss of generality, this model can be used to estimate the battery lifetimes for other applications too, especially those applications where the battery cycling undergoes cycling at similar C-rates as those of SHS.
6. **Usefulness at battery level.** Most performance-based experimentally constructed models are based on cell-level experiments, and the same battery technology might exhibit different characteristics at the battery level. With the proposed model, one can pick a candidate battery product and proceed to estimate the battery lifetime at the system design stage.

4. Results and discussions

4.1. Battery usage

The battery experiences a wide range of DOD levels due to the intermittent nature of the incident solar irradiance on the SHS and the varying load profile. This can be seen from Fig. 9 that shows the normalized frequency of the different DOD levels throughout the year for the lead-acid gel battery under 2 cases, viz. considering the overall battery DOD data and only the active battery DOD data.

The active battery data points were considered based on the zero-crossings, as described in Section 3.3.2. As seen in Fig. 9, the two different cases differ in their DOD levels. Between 10% and 70% DOD the active DOD occur relatively more frequently. However, in the very shallow (0–10%), and very deep DODs (70–80%), the trend is reversed, showing a lesser occurrence of active DODs, underlining the periods of inactivity of the battery. This corresponds to when the battery was either full (not needed to power the load) or empty (could not power the load). Moreover, the maximum limit of the DOD shown in the histogram is 80%, owing to the lower limit of the battery SOC fixed at 20% in the simulation.

Additionally, the battery cycling related data is extracted using both the coarse average and the ZCs approach. The results are shown in Table 2.

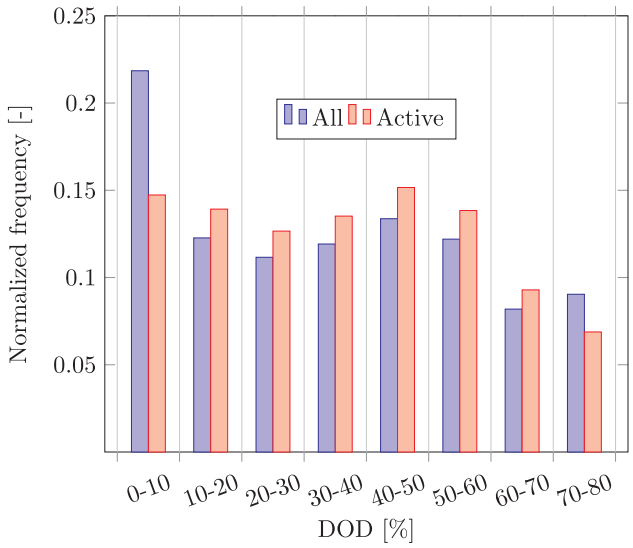

Fig. 9. Normalized frequency of the DODs experienced by the lead-acid gel battery for both the overall battery DOD data and only the active battery DOD data.

Table 2
Usage statistics for the 4 battery technologies over 1 year of SHS simulation. LA: lead-acid, CA: Coarse average based, ZC: Zero crossings based.

Battery	$\overline{DOD}$ (%)		$\overline{T}$ (°C)		E_{thr}
	CA	ZC	CA	ZC	(kWh/ year)
Flooded LA	37.81	38.21	27.16	26.94	613.9
LA gel	36.23	36.73	27.16	26.78	589.7
NiCd	39.77	40.04	27.16	27.2	647.7
$LiFePO_4$	35.11	35.66	27.16	26.7	575.7

A difference can be seen across the 4 battery technologies for the various battery parameters. In general, the coarse average-based DOD is more optimistic than the ZCs-based DOD for all the technologies. The difference in the DOD using the same method for different batteries comes from the fact that the different batteries have different operating efficiency, and therefore need to cycle differently in order to meet the storage demand of the given SHS application. Similarly, the energy throughputs of the different battery technologies are also different. The coarse-average temperature is the same for every battery technology based on the meteorological data, while the ZCs-based temperature is slightly different, depending on the duration of the ZC-cycles (refer Eq. (8)), which differ across technologies.

$LiFePO_4$ fares the best across the different battery statistics, while the NiCd battery fares the worst. Lead-acid gel battery performs slightly better than its flooded counterpart. In general, the more efficient the battery, the lower the DOD as well as temperature and energy throughput for the exact same application. Consequently, the cycle life will also be higher than that of a battery with lower efficiency, as seen in Section 4.2 below.

Even though the average DOD values between the two methods differ only by about 1–1.5%, this difference can be significantly amplified based on the battery size chosen and the SHS load requirements. For example, oversizing the battery (lower LLP) would have resulted in a larger difference between the coarse average and the ZCs-based active DOD calculations. Going forward, the more conservative ZCs-based battery lifetime results are discussed, as using a coarse average-based estimation can yield to an optimistic prediction of battery lifetime.

Table 3
Cycle life and battery lifetime in years, based on the overall battery usage based lifetime estimation. LA: Lead-acid.

Technology	Cycle life (–)	Lifetime (years)
Flooded LA	3329	6
LA gel	3796	6.8
NiCd	1662	3
$LiFePO_4$	16,450	29.4

4.2. Lifetime estimation

Based on the battery usage discussed in Section 4.1, the battery lifetime is estimated based on the methodologies described in Section 3.

4.2.1. Overall battery usage based lifetime estimation

The results for the overall battery usage-based estimated lifetimes are shown in Table 3.

Following the battery usage statistics discussed in Section 4.1, the battery lifetime follows a similar relative trend. $LiFePO_4$ comprehensively outperforms the other battery technologies, having an estimated battery lifetime of nearly 5 times the lead-acid batteries and almost 10 times the NiCd battery.

4.2.2. Dynamic lifetime estimation

Based on the dynamic lifetime estimation method described in Section 3.4, the battery lifetimes for the SHS use-case were estimated for the 4 battery technologies. The results for the dynamic capacity fading based lifetime estimation are shown in Fig. 10. For comparison, the results from the overall battery usage based estimation method are also plotted.

As seen in Fig. 10, the dynamic lifetime estimation is found to be much more conservative, with lifetimes for LA-gel, LA-flooded, NiCd, $LiFePO_4$ batteries as 5.6, 5.1, 2.86, and 16.7 years, which are 18%, 14%, 3%, and 43% less than the corresponding overall usage based lifetime estimates, respectively. This is attributed to the fact that dynamic lifetime degradation captures the micro-degradation of the battery capacity for every micro-cycle. Consequently, the battery is progressively degraded as it enters the next micro-cycle with a faded capacity, instead of calculating the lifetime based on overall usage of one year where the battery performs identically without any degradation. Therefore, the dynamic capacity fading model-based lifetime estimation is considered more practical and realistic. Additionally, the longer the battery lasts, the more pronounced effect of dynamic capacity fading. Therefore, from NiCd to $LiFePO_4$ the deviation from the

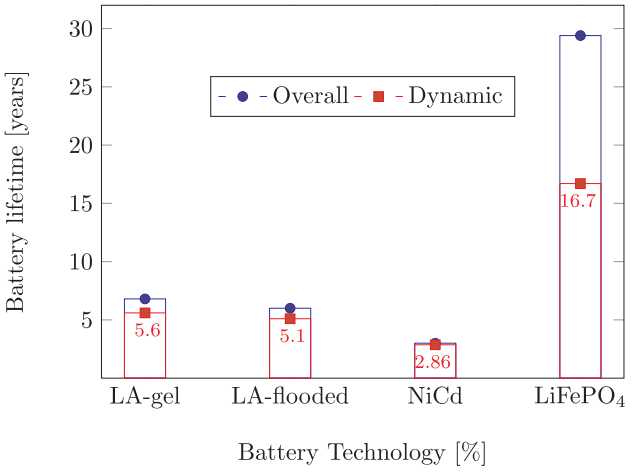

Fig. 10. Dynamic battery lifetime estimation results for the 4 battery technologies in comparison with the results using the overall battery usage method.

overall battery lifetime estimation method is increasing.

Of course, it must be noted that the methodology described here relies on the manufacturer's datasheet, and therefore the relative lifetime estimation for this particular SHS application need not be extendable to all battery products from the same technology. This is because different battery products from the same technology often display varying cycle lives depending on the construction geometry, propriety manufacturing processes, amongst others.

A comparison of this model is also made with an experimentally obtained empirical model for capacity fading of $LiFePO_4$, as explained in Section 4.3.

4.3. Comparison with an empirical battery lifetime estimation model

As an experimental validation of the dynamic lifetime estimation model can take an impractically long time, the accuracy of the model was compared to the results obtained from another experimentally created, empirical-based lifetime estimation model based on $LiFePO_4$ battery technology as described in [41]. The empirical model can been described by Eqs. (12) and (13) [41].

$$cf = \sum_{i}^{E} \left((k_{s1} SOC_{dev,i}. \, e^{k_{s2}.SOC_{avg,i}} + k_{s3}. \, e^{k_{s4}.SOC_{dev,i}}). \, e^{\left(-\frac{E_g}{R}\left(\frac{1}{T_i}-\frac{1}{T_{ref}}\right)\right)} \right) Ah_i \tag{12}$$

where cf is the capacity fading experienced by the battery due to all the cycling events E, i is an event for an arbitrary length of time, Ah_i is the total charge processed during event i, E is the total number of events.

The temperature dependence term comes from the Arrhenius equation, where k_{s1} to k_{s4} are constants determined experimentally and reported in [41], $SOC_{dev,i}$ is the normalized standard deviation from SOC_{avg} in event i. This value is derived from Eq. (13) [3].

$$SOC_{dev} = \sqrt{\frac{3}{\Delta Ah_m} \int_{Ah_{m-1}}^{Ah_m} (SOC(Ah) - SOC_{avg})^2 . \, dAh} \tag{13}$$

To be applied in the SHS application discussed in this study, Eq. (12) was adapted to the battery usage obtained in the SHS use-case. Similar to the approach discussed in Section 3.4, the capacity fading was calculated per cycling event (ZC micro-cycle) with the help of Eqs. (12) and (13). Consequently, the battery lifetime was found to be 14.3 years, about 14.2% deviation from the dynamic battery lifetime estimation method.

The State of Health (SOH) is also calculated based on the empirical method, which is discussed along with the other SOH results in Section 4.3.1 below.

4.3.1. State of Health (SOH)

While the lifetime results mentioned above give a measure of the overall battery life for the given application, the SOH results over time give a measure of the rate of the capacity fading for different battery technologies. For the given battery lifetime estimation modelled in this study, the State of Health (SOH) was computed for the different batteries under operating conditions, i.e., taking only cyclic ageing into account.

The results are plotted in Fig. 11. For the same starting battery capacity, the slowest fading rate is seen to be experienced by the $LiFePO_4$ battery, while the fastest rate (steepest slope) is experienced by the considered NiCd battery. The SOH results seem to show a near-linear trend over time.

Additionally, the SOH is plotted for the empirical lifetime estimation model for the same SHS use-case considered, as shown in Fig. 11. The SOH from the empirical model follows the dynamic lifetime estimation method-based SOH (both for $LiFePO_4$) closely, especially up to 89% SOH. After year 10, the SOH estimates start to deviate. The SOH deviations at the various year-marks differ by a maximum of 2.8%. However, it must be noted that the comparison with empirical model is only valid for the $LiFePO_4$ battery technology and as such the degree of accuracy shown by this comparison cannot be extended to other technologies solely on this basis. No empirical models were found for the other technologies at the time of writing this article, which could enable a similar comparison for the SHS use-case for the exact same stress factors as considered in the proposed methodology.

In summary, the main difference between the 2 proposed models, viz. the overall usage model, and the dynamic capacity fading model, is the increased complexity and accuracy of the dynamic capacity fading model. Within the overall battery usage model, the coarse average approach is rather crude but quick, while the ZC micro-cycle based approach is more computationally demanding. However, the overall battery usage model is not without its assumptions, as discussed in Section 3.3.3. The dynamic capacity fading model is the most complex but remarkably matches the experimentally derived empirical model until about 89% SOH.

4.4. Relevance for SHS design

In the context of SHS application, the battery lifetime estimation exercise is quite relevant, as explained in Section 1. This is even more relevant in the off-grid electrification segment, where system reliability plays a critical role in technology adoption. This study was extended to investigate the impact of SHS battery sizing on battery lifetime to underline the importance of estimating battery lifetime at the SHS design stage.

Fig. 12 shows the impact of battery sizing on battery lifetime for the same SHS use-case as considered in the rest of the study. The battery lifetime was evaluated using dynamic battery lifetime estimation methodology described in Section 3.4 for a range of battery sizes from 100 Wh (severely undersized) to 4 kWh (nearly 3 times oversized). The curve is seen to taper at the lower end in the beginning; this is because the battery is significantly undersized, and the SHS cycles the battery completely to meet the load demand. A linear trend can be seen in the lifetime with increasing battery size for the middle range of battery sizes. Towards the end of the battery, the lifetime increase is slower. Thus, the largest benefit of oversizing the battery is clearly seen only after around 1 kWh and up to around 3 kWh.

Compared to a typical PV module that lasts 25 years, an SHS battery usually lasts much less. Therefore, the battery will need to be replaced in the SHS lifetime. Fig. 12 also explores the number of replacements needed as the battery size changes for the same SHS application. As can be seen, a larger battery size not only increases the lifetime but also

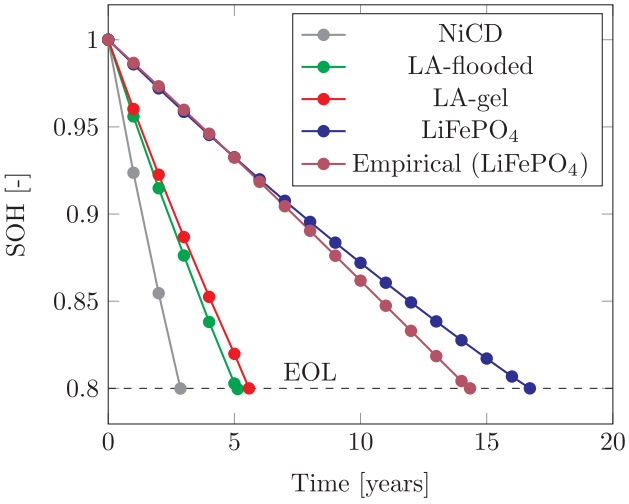

Fig. 11. SOH for the different battery technologies as estimated by the dynamic lifetime method. The black dashed line denotes the end of life.

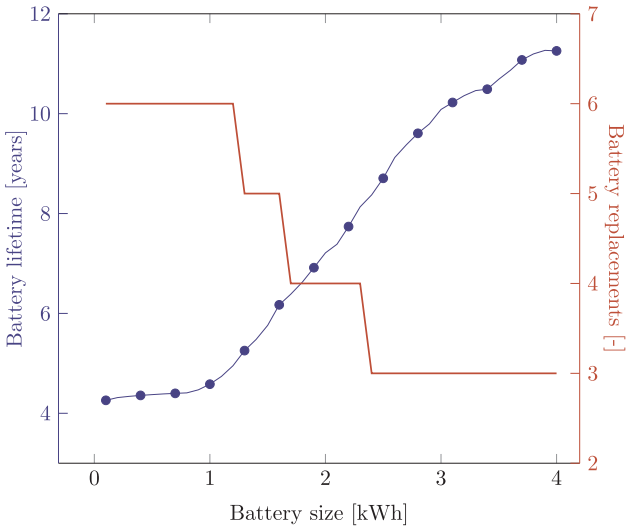

Fig. 12. Variation of battery lifetime with battery size for the lead-acid gel battery under the same load profile and PV size (Wp).

consequently reduces the number of battery replacements needed in the SHS lifetime. This presents an interesting trade-off between the upfront costs and battery replacement costs; the cost of having an increased lifetime (and therefore increased battery size) for the same application is the increased upfront costs that come along with a larger battery size. Therefore, estimating the battery lifetime at the SHS design stage can help optimize this delicate trade-off between upfront costs and battery replacement costs. Additionally, based on the technology learning curves, the decreasing battery technology costs and discounting the future costs, it can make for an interesting optimization study to select the best technology and size for a given SHS application for instance. Although not part of our specific study, it is recommended to have deeper research for exploring this further.

It must be noted that in the range of battery size considered in Fig. 12, the SHS load demand will be satisfied to different levels, as illustrated in the results of the LLP analysis shown in Fig. 6. Therefore, the battery sizes lower than fixed size (1440 Wh) will lead to LLP values significantly higher than 1.8%.

5. Conclusion

This paper described a practical methodology for estimating the battery lifetime without needing to model the electrochemical processes within the battery or needing dedicated experiments. Moreover, this methodology uses available battery data from the manufacturer for candidate battery technologies at hand. The methodology is applicable irrespective of the battery technology, as it is independent of the technology-specific electro-chemical processes. The methodology can also be extended to other applications experiencing similar battery C-rates without loss of generality. The described methodology is expected to help SHS designers make informed decisions with respect to the battery storage at the system sizing stage.

Dynamic capacity fading model introduced in this paper was deemed more practical than the overall battery usage model. For a given load profile and specific SHS system size, the estimated lifetimes for LA-gel, LA-flooded, NiCd, $LiFePO_4$ batteries were 5.6, 5.1, 2.86, and 16.7 years, respectively using the dynamic capacity fading model. Comparison of this proposed dynamic model with an experimentally derived empirical model of $LiFePO_4$ battery yielded very close results, with the SOH values over time being within 2.8%. Additionally, the impact of SHS battery sizing on battery lifetime was investigated, showing that higher upfront costs due to a large battery size could be used to offset the replacement costs through increased battery lifetime.

Future work

The study described in this paper uses constant average efficiency values for the various battery technologies. As the battery degrades, the battery performance in terms of efficiency and other parameters like internal resistance is also expected to degrade. Further study is identified and underway to include the efficiency variation for quantifying battery performance degradation along with capacity fading.

Acknowledgment

This work is supported by a fellowship from the Delft Global Initiative of the Delft University of Technology. The authors thank Vasilis Marioleas and Yunizar Pragistio.

References

[1] Narayan N, Popovic J, Diehl JC, Silvester S, Bauer P, Zeman M. Developing for developing nations: exploring an affordable solar home system design. 2016 IEEE global humanitarian technology conference (GHTC) 2016. p. 474–80. https://doi.org/10.1109/GHTC.2016.7857322.

[2] Palit D, Bandyopadhyay KR. Rural electricity access in South Asia: Is grid extension the remedy? A critical review. Renew Sustain Energy Rev 2016;60:1505–15.

[3] Narayan N, Papakosta T, Vega-Garita V, Popovic-Gerber J, Bauer P, Zeman M. A simple methodology for estimating battery lifetimes in solar home system design. 2017 IEEE AFRICON 2017. p. 1195–201. https://doi.org/10.1109/AFRCON.2017.8095652.

[4] IEA. World Energy Outlook 2016. 1st ed. Organization for Economic Cooperation and Development. International Energy Agency; 2016.

[5] Initiative GS. Quality charter: quality standards for accredited solar suppliers, good solar initiative; 2016. < http://www.goodsolarinitiative.org/uploads/2/4/8/5/24859908/good_solar_initiative_-_quality_charter_-_24mar2015_-_final_approved.pdf > .

[6] Phadke AA, Jacobson A, Park WY, Lee GR, Alstone P, Khare A. Powering a home with just 25 watts of solar pv. Super-efficient appliances can enable expanded off-grid energy service using small solar power systems. Tech. rep. Berkeley, CA (United States): Lawrence Berkeley National Laboratory (LBNL); 2015.

[7] Heeten TD, Narayan N, Diehl JC, Verschelling J, Silvester S, Popovic-Gerber J, et al. Understanding the present and the future electricity needs: consequences for design of future solar home systems for off-grid rural electrification. 2017 International conference on the domestic use of energy (DUE) 2017. p. 8–15. https://doi.org/10.23919/DUE.2017.7931816.

[8] Zou C, Manzie C, Neic D, Kallapur AG. Multi-time-scale observer design for state-of-charge and state-of-health of a lithium-ion battery. J Power Sources 2016;335:121–30. https://doi.org/10.1016/j.jpowsour.2016.10.040<https://www.sciencedirect.com/science/article/pii/S037877531631432X>.

[9] Zou C, Hu X, Wei Z, Tang X. Electrothermal dynamics-conscious lithium-ion battery cell-level charging management via state-monitored predictive control. Energy 2017;141:250–9. https://doi.org/10.1016/j.energy.2017.09.048<http://www.sciencedirect.com/science/article/pii/S0360544217315712>.

[10] Zou C, Hu X, Wei Z, Wik T, Egardt B. Electrochemical estimation and control for lithium-ion battery health-aware fast charging. IEEE Trans Ind Electron 2018;65(8):6635–45. https://doi.org/10.1109/TIE.2017.2772154.

[11] Marano V, Onori S, Guezennec Y, Rizzoni G, Madella N. Lithium-ion batteries life estimation for plug-in hybrid electric vehicles. 2009 IEEE vehicle power and propulsion conference 2009. p. 536–43. https://doi.org/10.1109/VPPC.2009.5289803.

[12] Dubarry M, Liaw BY, Chen M-S, Chyan S-S, Han K-C, Sie W-T, et al. Identifying battery aging mechanisms in large format li ion cells. J Power Sources 2011;196(7):3420–5. https://doi.org/10.1016/j.jpowsour.2010.07.029<http://www.sciencedirect.com/science/article/pii/S0378775310012127>.

[13] Agarwal V, Uthaichana K, DeCarlo RA, Tsoukalas LH. Development and validation of a battery model useful for discharging and charging power control and lifetime estimation. IEEE Trans Energy Convers 2010;25(3):821–35. https://doi.org/10.1109/TEC.2010.2043106.

[14] Dufo-López R, Lujano-Rojas JM, Bernal-Agustn JL. Comparison of different lead-acid battery lifetime prediction models for use in simulation of stand-alone photovoltaic systems. Appl Energy 2014;115:242–53. https://doi.org/10.1016/j.apenergy.2013.11.021<http://www.sciencedirect.com/science/article/pii/S0306261913009148>.

[15] Tankari MA, Camara MB, Dakyo B, Lefebvre G. Use of ultracapacitors and batteries for efficient energy management in wind-diesel hybrid system. IEEE Trans Sustain Energy 2013;4(2):414–24. https://doi.org/10.1109/TSTE.2012.2227067.

[16] Musallam M, Johnson CM. An efficient implementation of the rainflow counting algorithm for life consumption estimation. IEEE Trans Reliab 2012;61(4):978–86. https://doi.org/10.1109/TR.2012.2221040.

[17] Dragičević T, Pandžić H, Skrlec D, Kuzle I, Guerrero JM, Kirschen DS. Capacity optimization of renewable energy sources and battery storage in an autonomous telecommunication facility. IEEE Trans Sustain Energy 2014;5(4):1367–78. https://doi.org/10.1109/TSTE.2014.2316480.

[18] Layadi TM, Champenois G, Mostefai M, Abbes D. Lifetime estimation tool of lead-acid batteries for hybrid power sources design. Simul Model Pract Theory 2015;54:36–48. https://doi.org/10.1016/j.simpat.2015.03.001 < http://www.sciencedirect.com/science/article/pii/S1569190X15000362 > .
[19] für Sonnenenergie DG. Planning and installing photovoltaic systems: a guide for installers, architects and engineers, planning and installing. Taylor & Francis; 2008 < http://books.google.nl/books?id = fMo3jJZDkpUC > .
[20] Mohanty P, Muneer T, Mohan K. Solar photovoltaic system applications. Springer; 2016.
[21] Palacin MR, de Guibert A. Why do batteries fail? Science 2016;351(6273):1253292. https://doi.org/10.1126/science.1253292 < http://www.sciencemag.org/cgi/doi/10.1126/science.1253292 > .
[22] Keil P, Schuster SF, Wilhelm J, Travi J, Hauser A, Karl RC, et al. Calendar aging of lithium-ion batteries. J Electrochem Soc 2016;163(9):A1872–80. https://doi.org/10.1149/2.0411609jes < http://jes.ecsdl.org/lookup/doi/10.1149/2.0411609jes > .
[23] Lawder MT, Northrop PWC, Subramanian VR. Model-based SEI layer growth and capacity fade analysis for EV and PHEV batteries and drive cycles. J Electrochem Soc 2014;161(14):A2099–108. https://doi.org/10.1149/2.1161412jes < http://jes.ecsdl.org/content/161/14/A2099.abstract > .
[24] Ruetschi P. Aging mechanisms and service life of lead-acid batteries. J Power Sources 2004;127(1–2):33–44. https://doi.org/10.1016/j.jpowsour.2003.09.052.
[25] Brik K, Ben Ammar F. Causal tree analysis of depth degradation of the lead acid battery. J Power Sources 2013;228:39–46. https://doi.org/10.1016/j.jpowsour.2012.10.088.
[26] Viera JC, González M, Anton JC, Campo JC, Ferrero FJ, Valledor M. NiMH vs NiCd batteries under high charging rates. In: INTELEC, international telecommunications energy conference (proceedings). https://doi.org/10.1109/INTLEC.2006.251592.
[27] Wang J, Liu P, Hicks-Garner J, Sherman E, Soukiazian S, Verbrugge M, et al. Cycle-life model for graphite-LiFePO4 cells. J Power Sources 2011;196(8):3942–8. https://doi.org/10.1016/j.jpowsour.2010.11.134.
[28] Installation, commissioning and operating instructions for valve-regulated stationary lead-acid batteries - solar battery data sheet; 2015.
[29] Valence life — lithium ion phosphate battery manufacturer; 2017. < https://www.valence.com/why-valence/long-lifecycle/ > [date last accessed 2015-05-03].
[30] Installation, commissioning and operating instructions for vented stationary lead-acid batteries - solar battery data sheet; 9 2015.
[31] Alpha power - industrial ni-cd batteries standard range technical manual; 2009.
[32] Bhatia M, Nicolina A. Capturing the multi-dimensionality of energy access, live wire, 2014/16. World Bank, Washington, DC. ©World Bank; 2014. < https://openknowledge.worldbank.org/handle/10986/18677 > . License: CC BY 3.0 IGO.
[33] Global LEAP. The state of the off-grid appliance market. Tech. rep.; 2016. < http://www.cleanenergyministerial.org/Portals/2/pdfs/Global_LEAP_The_State_of_the_Global_Off-Grid_Appliance_Market.pdf > .
[34] GIZ. Photovoltaics for productive use applications - a catalogue of DC-appliances; 2016.
[35] Meteotest, (software) meteonorm ver 7.1; 2014.
[36] Dunn B, Kamath H, Tarascon J-m. Electrical energy storage for the grid: a battery of choices. Sci Mag 2011;334(6058):928–36. https://doi.org/10.1126/science.1212741.
[37] Van den Bossche P, Vergels F, Van Mierlo J, Matheys J, Van Autenboer W. SUBAT: an assessment of sustainable battery technology. J Power Sources 2006;162(2 SPEC. ISS.):913–9. https://doi.org/10.1016/j.jpowsour.2005.07.039.
[38] Hojckova K, Jelinek J, Schneider M, Spittler N, Varju I. Evaluation of battery storage technologies for sustainable and rural electrification in Sub-Saharan Africa. Regional Academy on the United Nations (RAUN); 2015. < http://www.ra-un.org/uploads/4/7/5/4/47544571/evaluation_of_battery_storage_technologies_1.pdf > .
[39] Luo X, Wang J, Dooner M, Clarke J. Overview of current development in electrical energy storage technologies and the application potential in power system operation. Appl Energy 2015;137:511–36. https://doi.org/10.1016/j.apenergy.2014.09.081.
[40] Herritty RM, Midolo J. Nickel cadmium batteries for photovoltaic applications. In: Thirteenth annual battery conference on applications and advances. Proceedings of the conference; 1998. p. 255–7. https://doi.org/10.1109/BCAA.1998.653876.
[41] Lam L. A practical circuitbased model for state of health estimation of liion battery cells in electric vehicles [Master's thesis]. Delft University of Technology; August 2011.